Available online at www.sciencedirect.com
ScienceDirect
Corrosion Science 49 (2007) 186–194
CORROSION SCIENCE
www.elsevier.com/locate/corsci

Recent advances on physico-chemical characterization of passive films by EIS and differential admittance techniques

F. Di Quarto *, F. La Mantia, M. Santamaria

Dipartimento di Ingegneria Chimica, dei Processi e dei Materiali, Università di Palermo, Viale delle Scienze, 90128 Palermo, Italy

Available online 17 July 2006

Abstract

Thin Nb_2O_5 anodic films (~20 nm thick) grown in phosphoric acid solution have been characterised by EIS and differential admittance study in a large range of potential and frequency. The overall electrical behaviour has been interpreted by means of the theory of amorphous semiconductor Schottky barrier in presence of a non-constant density of states (DOS). A comparison of DOS for films grown in different electrolytes is reported.

Keywords: A. Passive film; B. a-SC Schottky barrier; C. EIS spectra

1. Introduction

The physico-chemical characterisation of passive films and corrosion layers is a long task aimed to the comprehension of the corrosion behaviour of metals and alloys. In this frame the study of electronic properties of passive films is a challenge owing to their complex nature if compared with bulk crystalline materials. The importance of electronic properties of passive films in determining the kinetics of charge transfer at the passive film/electrolyte interface has been stressed in a previous paper [1].

* Corresponding author. Tel.: +39 091 6567228; fax: +39 091 6567280.
E-mail address: diquarto@unipa.it (F. Di Quarto).

0010-938X/$ - see front matter
doi:10.1016/j.corsci.2006.05.019

Electrochemical impedance spectroscopy (EIS) and capacitance as a function of electrode potential ($C(\omega)$ vs U_E) measurements are very popular techniques in corrosion studies in providing useful information on the structure of passive film-electrolyte interface as well as on electronic properties of passive films and corrosion layers grown on metals and alloys.

In an attempt to overcome the limitations of Mott–Schottky approach in the study of semiconducting passive films we proposed years ago a different approach based on the theory of amorphous semiconductor (a-SC) Schottky barrier in the low band bending regime [2].

More recently we have tried to extend such an approach to the high band bending regime by taking into account the possible influence of a non constant distribution (both in energy and spatially) of electronic density of states (DOS) [1,3].

In this paper the use of EIS spectra and differential admittance (DA) plots ($Y_{a\text{-}SC}$ vs U_E) for investigating a-SC Schottky barriers, in high band bending regime and in presence of a non-constant DOS, will be highlighted. A study on the solid state properties of amorphous [4,5] semiconducting thin (about 20 nm) a-Nb_2O_5 films grown in phosphoric acid solution will be carried out. Moreover a comparison of solid state properties of amorphous Nb_2O_5 passive films grown in different solutions (H_2SO_4, H_3PO_4, NaOH) will be presented and discussed.

2. Amorphous vs crystalline semiconductor Schottky barrier: a short theoretical background

For sake of brevity details of theory of amorphous semiconductors (a-SC) and a-SC Schottky barrier will be largely omitted here. The interested readers can benefit of the original literature reported in Refs. [6,7]. In the following we summarise the main aspects of a-SC Schottky barrier theory whilst as for the derivation of final equations and equivalent circuit employed for fitting EIS and DA curves of a-Nb_2O_5/electrolyte junctions further details can be found in a very recent work [3].

According to the theory [6,7] the main differences in admittance behaviour of crystalline SC and a-SC can be traced out to the presence of a finite DOS within the mobility gap ($E_C - E_V$) of a-SC. The conduction (E_C) and valence band (E_V) mobility edges separate, respectively, the region of extended electronic states (above E_C or below E_V) from the localised ones (between E_C and E_V). Such a DOS distribution affects noticeably the shape of space charge barrier as well as the frequency response of a metal/a-SC Schottky barrier. This is evidenced in Fig. 1 where the energetics of n-type a-SC/El junction, with simplifying hypothesis of constant DOS and spatially homogeneous material, is reported. The main difference with respect to the case of crystalline SC is that the net space charge depends on both the ionized impurities and occupied localised states within the mobility gap. By assuming an exponential relationship for the capture-emission process of electrons from a localized state as:

$$\tau = \tau_0[\exp(E_C - E/kT)] \tag{1}$$

it has been shown that it is possible to define a cut-off energy level, E_ω, which separates states fully responding from those not responding at all to the ac signal, by using the condition: $\omega\tau = 1$ [2,3].

According to the previous equation it follows that:

$$E_C - E_\omega = -kT\ln(\omega\tau_0) \tag{2}$$

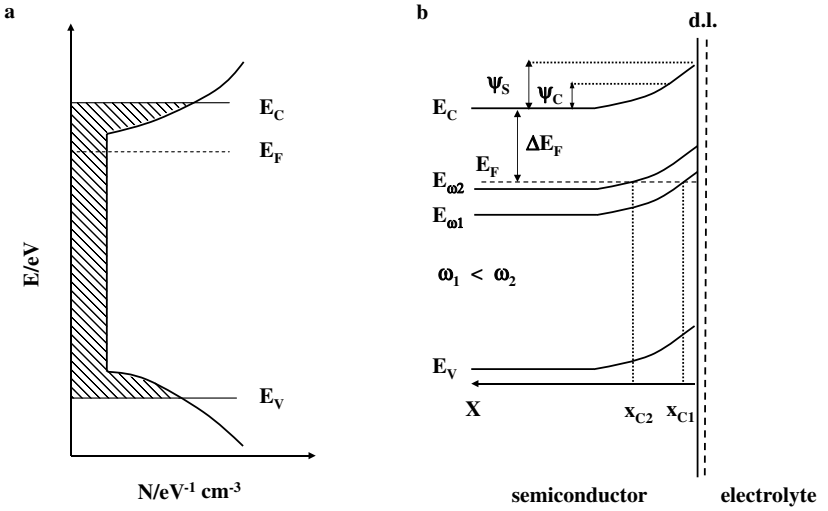

Fig. 1. (a) Schematic DOS distribution in a-SC. (b) Energetics of a-SC/El junction. The dashed area evidences localized electronic states.

where, at constant temperature, τ_0 is a constant characteristic of each material usually ranging between $10^{-14} - 10^{-10}$ s. With reference to Fig. 1 the intersection of E_ω with the Fermi level of material marks a characteristic point inside the barrier, X_C, corresponding to a band bending ψ_C defined by:

$$|e|\psi_C = |e|\psi(X_C) = -kT\ln(\omega\tau_0) - \Delta E_F \tag{3}$$

where $\Delta E_F = (E_C - E_F)_{bulk}$. X_C is now a distance in the barrier which changes with changing frequency, ω, and band bending $\psi_S = U_E - U_{fb}$. In particular X_C increases with increasing frequency, at constant polarization, or with increasing polarization at constant frequency. From the theory it comes out that [6,7]:

- at low band bending ($\psi_S < \psi_g = eV_g = (E_g/2 - \Delta E_F)$) the total capacitance is sum of two series contribution coming from the $X < X_C$ and $X > X_C$ regions of the a-SC;
- at high band bending regime ($\psi_S > \psi_g = eV_g = (E_g/2 - \Delta E_F)$), when a deep depletion region (HBB) appears at the surface of a-SC/El junctions, a third term (frequency independent) representing the capacitance of the deep depletion region must be added to the total capacitance [3];
- in both cases the contribution to the conductance comes from the region around $X = X_C$ dividing the total response from null response regions.

In the hypothesis of constant DOS, N, and HBB, the following analytical expressions for both components of differential admittance, $Y_{a\text{-}SC}$, can be derived [1,3]:

$$\frac{1}{C_{HBB}(\omega,\psi_S)} = \frac{1}{\sqrt{\varepsilon\varepsilon_0 e^2 N}}\left(\ln\frac{\psi_g}{\psi_C} + \sqrt{1 + \frac{2}{V_g}(U_E - (U_{FB} + V_g))}\right) \tag{4}$$

$$G_{HBB}(\omega,\psi_S) = \pi^2 f \frac{kT}{|e|\psi_C}\sqrt{\varepsilon\varepsilon_0 e^2 N}\left(\ln\frac{\psi_g}{\psi_C} + \sqrt{1 + \frac{2}{V_g}(U_E - (U_{FB} + V_g))}\right)^{-2} \tag{5}$$

Table 1
Parameters used to fit EIS spectra of a-Nb_2O_5 film grown in 0.1 M H_3PO_4 solution up to 5 V(SCE)

U_e [V_{NHE}]	R_s [Ω cm^2]	C_{dl} [F/cm^2]	R_{ct} [Ω cm^2]	W [S/cm^2]	C_{ss} [F/cm^2]	Q [S/cm^2]	n	G_{ss} [S/cm^2]
0.19	0.5	2.00E−05	2.50E+02	4.20E−04	5.70E−04	7.20E−05	0.15	1.50E−05
0.41	0.5	2.00E−05	4.80E+02	4.20E−04	1.20E−04	4.40E−05	0.15	1.50E−06
0.5	0.5	2.00E−05	5.00E+02	4.20E−04	9.00E−05	4.40E−05	0.15	1.00E−06
1.0	0.5	2.00E−05	7.00E+02	4.20E−04	3.80E−05	3.50E−05	0.15	2.00E−06
2.0	0.5	2.00E−05	1.50E+03	∞	1.60E−05	3.00E−05	0.15	2.80E−06
3.0	0.5	2.00E−05	1.10E+03	∞	1.05E−05	2.60E−05	0.15	2.20E−06
4.0	0.5	2.00E−05	1.10E+03	∞	7.20E−06	2.45E−05	0.15	2.20E−06

Eqs. (4) and (5) have been derived under conditions: $\psi_S > \psi_C > 3kT/e$ and they coincide with the LBB expression for $\psi_S \leqslant \psi_g$ [1–3]. As reported in Refs. [6,7] the previous equations should be valid also in presence of a DOS variable with energy provided that changes in DOS are small within kT eV.

As for EIS spectra of a-Nb_2O_5/electrolyte interface it has been previously shown [3] that they could be fitted, in a wide range of frequencies (0.1 Hz $\leqslant f \leqslant$ 100 kHz) and electrode potentials, by using an electrical circuit including:

– a Randles equivalent circuit which account for the solution resistance, double layer capacitance and a charge transfer resistance R_{ct} in series with;
– a parallel $Y_{a\text{-}SC}//Y_{SS}$ circuit accounting for the contribution coming from a-SC space region and surface states (SS) admittance respectively.

In some cases (see Table 1) to fit EIS spectra at lower potentials a Warburg element in series with R_{ct} was added. When this occurred we suspect that it was an experimental artifact derived from an imperfect sealing of the lateral surface of metal rod allowing some peeling of electrolytic solution trough the electrical insulation.

3. Experimental

Electropolished niobium (purity 99.9) rod (Goodfellow Metals, Cambridge) was used for the experiments [3]. The metal was anodized at constant growth rate (10 mV s^{-1}) in 0.1 M H_3PO_4 ($U_F \leqslant$ 5 V/SCE) using a potentiostat (EG&G PAR 173) equipped with a function generator (EG&G PAR 175), and kept for 2 h to the formation voltage (stabilization). The same initial surface treatment was employed for films anodized in 0.1 M NaOH or 0.5 M H_2SO_4.

The impedance spectra and differential admittance curves were recorded by using a Parstat 2263 (PAR), connected to a computer for the data acquisition. For all the experiments a Pt net having a very high surface area was used as counter electrode. Unless differently stated all measurements reported below pertain to films formed in 0.1 M H_3PO_4 solution.

4. Results and discussion

Anodising ratio ranging between 26.5 and 26.8 Å V^{-1} were measured from the slope of C^{-1} vs U_E plots for film grown, at constant growth rate of 10 mV s^{-1}, in acidic as well as in

alkaline solution by using a dielectric constant for a-Nb_2O_5 equal to 42. After stabilisation, at $U_E = 5$ V/SCE, a film thickness of 19.3 nm was estimated for films grown in acidic solution. A slightly larger thickness (21 nm) was assigned to the film grown in NaOH solution by taking into account the shift with the solution pH of the equilibrium potential of the reaction:

$$Nb + 5H_2O = Nb_2O_5 + 10H^+ + 10e$$

The estimated thickness are in agreement with the data reported in literature for films grown at constant potential [4,5,8].

4.1. EIS Data Analysis

Stabilised a-Nb_2O_5 anodic films were investigated by EIS technique in a wide range of electrode potentials and frequency (0.1 Hz–100 kHz) by following the same procedure discussed in ref. [3]. In Fig. 2 we report the impedance spectra at different potentials, in Bode representation, of a-Nb_2O_5/H_2SO_4 junction for a film grown in 0.1 M H_3PO_4. The EIS spectrum as well as the shape of DOS used for fitting the EIS spectra are quite similar to that previously reported for film grown in 0.5 M H_2SO_4 solution [3]. This is confirmed by the results of Fig. 3 showing the Bode plots at the same potential of film formed in different solutions. The plots are almost overlapping in a large range of frequencies ($f > 3$ Hz) and start to display some differences at lowest employed frequencies. Further support comes from a comparison of data reported in Table 1, showing the values of the elements in the equivalent circuit used to fit the EIS spectra at different potentials, with corresponding data of film grown in H_2SO_4 [3] or in NaOH solution [9]. We like to stress that regardless of anodizing solution as for thin a-Nb_2O_5 film a good fitting of EIS spectra in the same range of investigated electrode potentials was obtained by using:

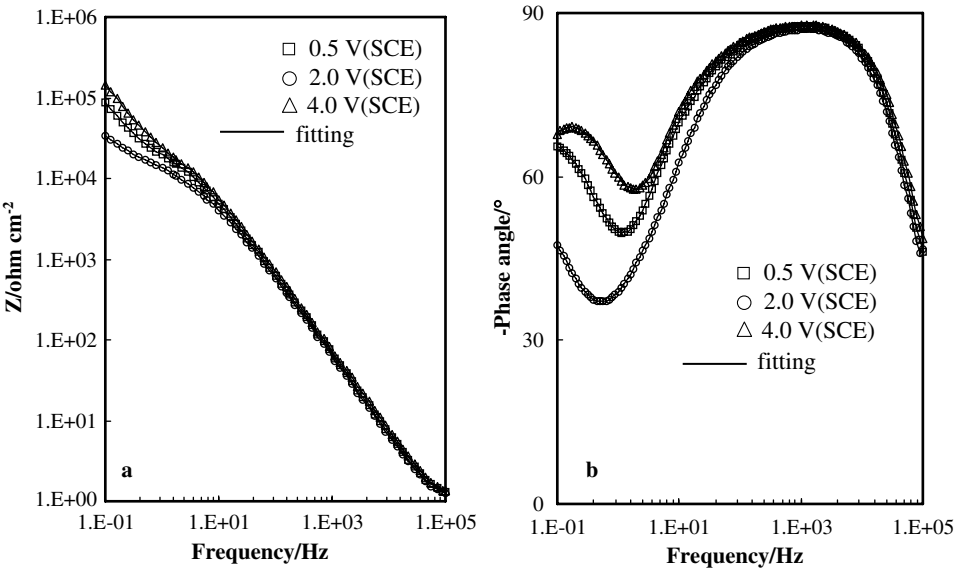

Fig. 2. Impedance spectra in the Bode representation at different potentials of a-Nb_2O_5/H_2SO_4 junction for a film grown in 0.1 M H_3PO_4 up to 5 V/(SCE) at 10 mV s^{-1} after stabilization.

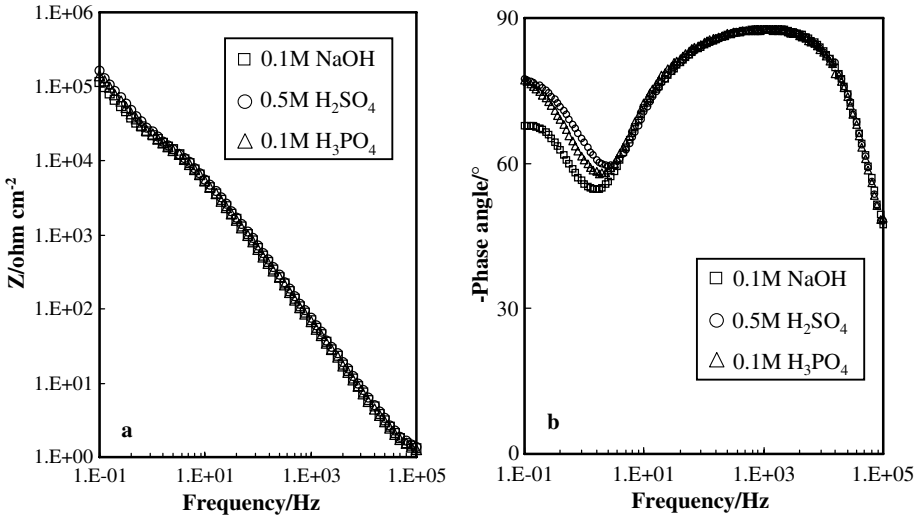

Fig. 3. Bode plots in 0.5 M H_2SO_4, at $U_E = 3$ V/SCE, for films grown up to 5 V (SCE) in different electrolytes.

- the same value of solution resistance ($\sim 0.5\ \Omega\ cm^2$) and Helmoltz double layer capacitance value ($\sim 20\ \mu F\ cm^{-2}$);
- a CPE ($Y_{CPE} = Q(i\omega)^n$) element, almost coincident with a resistor, displaying the same value of exponent ($n \approx 0.15$);
- values of G_{SS}, C_{SS} and Q not too far from those measured for film grown in 0.1 M H_3PO_4 solution.

All these findings suggest that the large difference in anion incorporation reported in literature [4,5] by anodising in sulphuric, phosphoric acid or NaOH solution is scarcely reflected in the fitting parameters of EIS spectra depending on the interfacial structure.

4.2. Differential Admittance Study

According to the results of EIS analysis and in agreement with the procedure described in previous study [3] the fitting of differential admittance curves was performed according to the equivalent circuit obtained by simple (series to parallel) transformations of the initial one. The data derived from fitting the EIS spectra were used for subtracting the Randles circuit and the equivalent $G_{p,SS}$ and $C_{p,SS}$ elements of the arm in parallel to a-SC Schottky barrier admittance.

The Y_{SC} vs U_E plots, derived with this procedure, were fitted by using the theoretical expressions for $C_{p,SC}$ and $G_{p,SC}$, obtained from the theory of a-SC Schottky barrier and modified as in ref. [3] for including possible spatial variation in DOS. According to this the following expression were used for fitting the two components of Y_{SC}:

$$\frac{1}{C_{p,SC}(x,\omega,\psi_S)} = \frac{1}{C_{p,SC}(\omega,\psi_S)} f_\omega(x(\psi_S)) \tag{6}$$

$$G_{p,SC}(x,\omega,\psi_S) = G_{p,SC}(\omega,\psi_S) g_\omega(x(\psi_S)) \tag{7}$$

where $f_\omega(x(\psi_S))$ and $g_\omega(x(\psi_S))$ are respectively two different trial functions depending only on the electrode potential but changing with employed frequency. The terms multiplying the two trial functions coincide with the expression of $(C_{p,SC})^{-1}$ and $G_{p,SC}$ in presence of a constant DOS (Eqs. (4) and (5)).

In Figs. 4(a) and (b) we report the experimental data as well as the fitting of admittance curves at different frequencies as a function of electrode potential for a film grown in H_3PO_4 solution. The value of ψ_C was kept constant in fitting both components of Y_{SC} but it changed with the frequency according to the constraint embodied in Eq. (3) and to an expected insulating behaviour of the film at an ac frequency around 200 kHz (where $\psi_C = 0$). In Fig. 5 we report the corresponding DOS distribution as a function of X_C derived from fitting the $G_{p\text{-}SC}$ vs U_E plots at different frequencies. Owing to the spectroscopic character of these plots it is possible to derive the spatial variation of DOS at the corresponding energy level $E_F - e\psi_C(\omega)$ [3].

On the other hand from the same curves, at different frequencies but a constant X_C (i.e., at fixed distance from oxide/electrolyte interface), it is possible to derive the DOS distri-

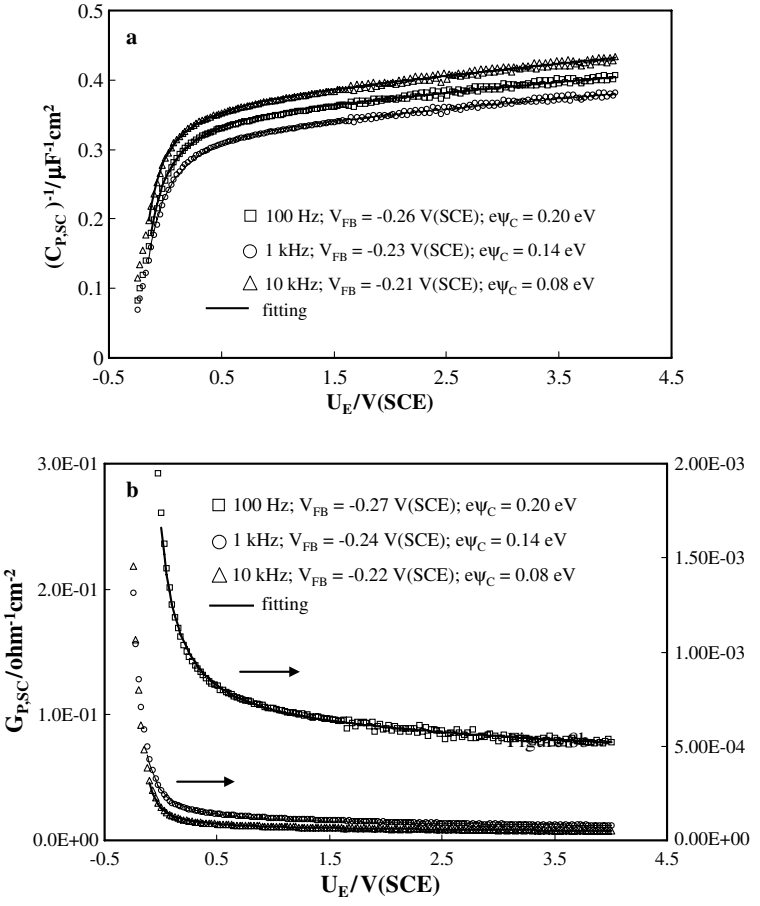

Fig. 4. (a) Fitting of $(C_{p,SC})^{-1}$ vs U_E and (b) $G_{p,SC}$ vs U_E curves at different frequencies as a function of electrode potential for a film grown in H_3PO_4 solution. Fitting parameter: Vg = 1.3 V at any frequency.

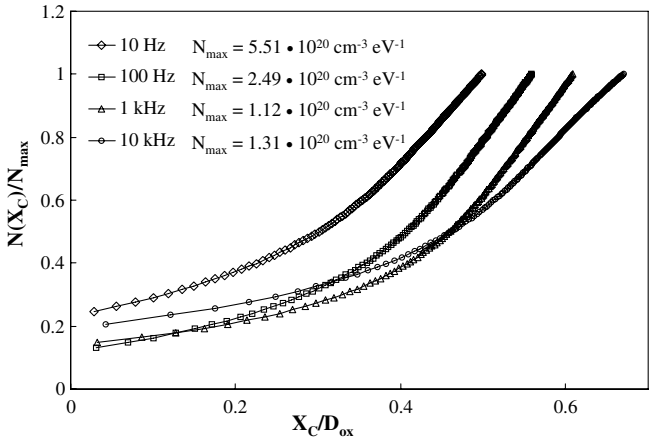

Fig. 5. Dimensionless DOS distribution as a function of X_C/D_{ox} derived from fitting the $G_{p,SC}$ vs U_E plots of Fig. 4 at different frequencies.

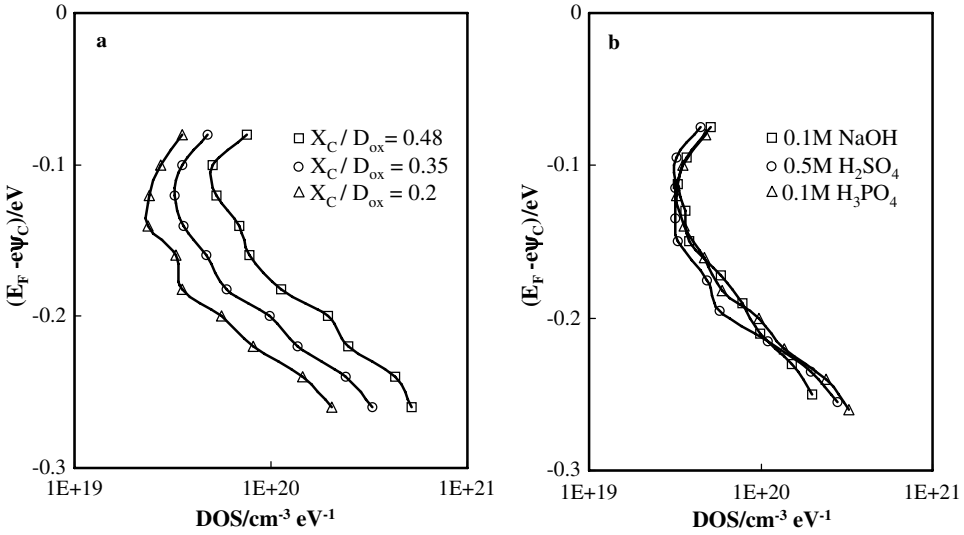

Fig. 6. (a) DOS distribution vs. energy for a film grown in H_3PO_4 solution at different values of X_C/D_{ox}; (b) DOS distribution vs. energy, at $X_C/D_{OX} = 0.35$, for films grown in different solutions up to 5 V/SCE.

bution as a function of energy (i.e., for any energy level $E_F - e\psi_C(\omega)$). The distribution of DOS vs energy derived from such a procedure is reported in Fig. 6(a) for three different values of X_C spanning a spatial region of film wide about 20% of total film thickness (distance from electrolyte/film interface ranging from 10 nm to 14 nm). Analogous plots in Fig. 6(b) for films grown in different solutions (H_2SO_4, H_3PO_4 and NaOH), at constant X_C, evidence a DOS distribution quite independent on the anodising electrolyte.

From the data of Figs. 5 and 6 it comes out that the DOS derived from fitting the DA curves changes with energy as well as with distance so confirming the overall behaviour

derived from EIS spectra and Eq. (3). The energy dependence of DOS appears as a general one because it has been previously observed also for semiconducting film grown on W and Ti metals [[3] and refs therein]. Such an energy dependence could be viewed as derived from an almost constant DOS summed up with a Gaussian distribution in energy of electronic states centred at around 0.35 eV from E_F. The origin of the energy as well as spatial DOS distribution could be related to presence of specific mobile defects, within the growing anodic film, which become frozen-in after stopping the anodisation process [10].

5. Conclusions

A study based on EIS spectra and differential admittance curves of a-Nb_2O_5/El interface in a large range of electrode potential and ac frequency has been carried out according to the theory of a-SC Schottky barrier. The DOS distribution for films grown in incorporating (H_2SO_4, H_3PO_4) and non-incorporating (NaOH) solution appears almost independent on the nature of anodizing solution. This finding suggests that the energy and spatial distribution of electronic DOS is probably related to the mechanism of growth and to the nature of mobile defects within the oxide film. In this frame the incorporation of sulphate and phosphate species could affect, eventually, the DOS deeper lying in energy. These results could help to have a better insight on the role of incorporated species on the electrical breakdown phenomena. Further studies are necessary to elucidate these aspects.

References

[1] F. Di Quarto, M. Santamaria, Corrosion Eng. Sci. Technol. 39 (2004) 71–81.
[2] F. Di Quarto, S. Piazza, C. Sunseri, Electrochim Acta 35 (1990) 99–107.
[3] F. Di Quarto, F. La Mantia, M. Santamaria, Electrochim Acta 50 (2005) 5090–5102.
[4] S. Ono, M. Baba, M. Shimiyama, H. Asoh, ECS PV 2003-25, V. Birss, L. Burke, A.R. Hillman, R.S. Lillard (Eds.), 2004, pp. 133–142.
[5] H. Habazaki, T. Ogasawara, H. Konno, K. Shimizu, K. Asami, K. Saito, S. Nagata, P. Skeldon, G.E. Thompson, Electrochim Acta 50 (2005) 5334–5339.
[6] J.D. Cohen, D.V. Lang, Phys. Rev. B 25 (1982) 5321–5350.
[7] W. Archibald, R.A. Abram, Phil. Mag. B 54 (1986) 421–438;
W. Archibald, R.A. Abram, Phil. Mag. B 56 (1987) 429–441.
[8] C.O.A. Olsson, M.G. Vergè, D. Landolt, J. Electrochem. Soc. 151 (2004) B652–B660.
[9] F. Di Quarto, F. La Mantia, M. Santamaria, in preparation.
[10] M.J. Dignam, Oxides and Oxide Films, Marcel Dekker, Inc., New York, 1 1972, pp. 91–286.